

## A Baseline Climatology of Sounding-Derived Supercell and Tornado Forecast Parameters

ERIK N. RASMUSSEN AND DAVID O. BLANCHARD

*Cooperative Institute for Mesoscale Meteorological Studies, National Severe Storms Laboratory and University of Oklahoma, Norman, Oklahoma*

(Manuscript received 21 November 1997, in final form 30 July 1998)

### ABSTRACT

All of the 0000 UTC soundings from the United States made during the year 1992 that have nonzero convective available potential energy (CAPE) are examined. Soundings are classified as being associated with nonsupercell thunderstorms, supercells without significant tornadoes, and supercells with significant tornadoes. This classification is made by attempting to pair, based on the low-level sounding winds, an upstream sounding with each occurrence of a significant tornado, large hail, and/or 10 or more cloud-to-ground lightning flashes. Severe weather wind parameters (mean shear, 0–6-km shear, storm-relative helicity, and storm-relative anvil-level flow) and CAPE parameters (total CAPE and CAPE in the lowest 3000 m with buoyancy) are shown to discriminate weakly between the environments of the three classified types of storms. Combined parameters (energy–helicity index and vorticity generation parameter) discriminate strongly between the environments. The height of the lifting condensation level also appears to be generally lower for supercells with significant tornadoes than those without. The causes for the very large false alarm rates in the tornadic/nontornadic supercell forecast, even with the best discriminators, are discussed.

### 1. Introduction

This paper establishes a baseline climatology of parameters commonly used in supercell thunderstorm forecasting and research. The climatology is derived from over 6000 soundings from 0000 UTC during 1992, all of which had nonzero convective available potential energy (CAPE) (Moncrieff and Miller 1976).

It is believed that a baseline climatology is needed to support certain aspects of operational thunderstorm forecasting. For example, values of CAPE are often cited in forecasts as being “marginal,” “large,” “extreme,” etc. However, no known baseline climatology exists that is adequate to support these quantifications for most of the commonly used parameters [except the climatology of Doswell and Rasmussen (1994) for CAPE]; rather, they generally are based on the subjective experience and “mental calibration” of the forecasters. Similar problems exist with the operational use of storm-relative helicity (SRH; Davies-Jones et al. 1990): what are climatologically large or extreme values of SRH? At what values should forecasters become concerned about mesocyclone potential?

There are a number of motivations for this study in the area of convection research. Because this is a 1-yr

climatology, it contains no information on the interannual variability of convection-related sounding-derived parameters. Thus, this study is suitable as a baseline for efforts to assess the interannual variability.

Another motivation is similar to the forecasting concerns mentioned above. Certain parameters have been established through theoretical or modeling work as being important in supercell structure, organization, etc. [e.g., the bulk Richardson number (Weisman and Klemp 1982), CAPE, SRH]. These parameters are then used in case studies and forecasting without thorough climatological verification. It is desirable to begin to assess the climatological occurrence of physically important parameters before they are proposed for use in operational meteorology. Conversely, it would seem to be desirable for those performing numerical modeling and theoretical studies to have data that indicate whether or not they are exploring physically relevant parts of a given parameter space.

It appears that there are no other sounding climatologies of this magnitude related to the environments of convective storms. Other investigations have focused more narrowly on various types of convection. For example, Maddox (1976) analyzed 159 proximity soundings to assess the effects of environmental winds on tornado production. In a similar study, Darkow and Fowler (1971) compared 53 tornado proximity soundings with “check” soundings farther away in the environment and found that winds were most noticeably

---

*Corresponding author address:* Dr. Erik N. Rasmussen, NSSL, 3450 Mitchell Lane, Building 3, Room 2034, Boulder, CO 80301.  
E-mail: rasmussen@nssl.noaa.gov

different in the 3–10-km layer. Much more exhaustive analyses of both wind and thermodynamic conditions near tornadic storms, and 6–12 h prior to their occurrence, can be found in Taylor and Darkow (1982) and Kerr and Darkow (1996).

Based on some of the foregoing studies, more recent work has tended to focus on SRH and other measures of lower-tropospheric shear, in combination with measures of potential buoyancy. In a limited sample, Rasmussen and Wilhelmson (1983) examined the combination of mean shear (related to hodograph length) and CAPE in the environments of tornadic, nontornadic severe, and nonsevere storms. As SRH increased in popularity as a forecast tool, climatological studies of sounding-derived parameters began to focus on combinations of CAPE and SRH (e.g., Davies 1993). Excellent summaries of the most recent climatological analyses of buoyancy and shear in the environments of tornadic storms can be found in Johns et al. (1993) and Davies and Johns (1993). An examination of helicity as a forecast tool is given by Davies-Jones et al. (1990), and Davies-Jones (1993) analyzed the mesoscale variation of helicity during tornado outbreaks using soundings from special sounding networks.

Sounding climatologies have also been used to assess the environments related to particular types of thunderstorms. Bluestein and Parks (1983) utilized soundings to compare the environments of low-precipitation storms and classic supercells, and Rasmussen and Straka (1998) investigated these and high-precipitation supercells using a sounding climatology. Bluestein and Parker (1993) have used soundings to investigate the modes of early storm organization near the dryline. A climatological sounding analysis of the environments associated with severe Oklahoma squall lines is reported in Bluestein and Jain (1985) and nonsevere squall lines in Bluestein et al. (1987).

In section 2, the methodology used in this climatological analysis is described, along with its limitations. Various parameter spaces are then investigated: shear (section 3), CAPE (section 4), combinations of CAPE and shear (section 5), and low-level thermodynamics (section 6). In section 7, the parameter space of Brooks et al. (1994a) is investigated. The forecast utility of the various parameters is compared in an objective manner in section 8. The results of this investigation are summarized in terms of tornadogenesis and supercell-favoring environments, and tornadogenesis failure modes, in section 9.

## 2. Methods

### a. Sounding database

The soundings evaluated here are contained in *Rawinsonde Data for North America, 1946–1992* (Forecast Systems Laboratory and National Climatic Data Center 1993) and were all made at 0000 UTC nominal sounding

time from the U.S. sites only. The year 1992 was chosen for this climatology in a completely arbitrary manner. The sounding data were subjected to two quality control checks only (beyond those performed in producing the CD-ROM dataset): hydrostatic checks and checks for missing wind data. Many soundings from 1992 have been examined using an interactive skew  $T$ - $\log p$  program, and no serious data problems have been encountered. Every sounding was evaluated for CAPE using the algorithm described below. If CAPE  $> 0$ , the sounding was further evaluated for a number of other parameters; 6793 soundings had nonzero CAPE and were utilized in this study.

### b. Proximity–inflow method

An objective method has been devised to associate each meteorological event with a sounding. A meteorological event is defined as a cloud-to-ground lightning flash or a severe weather report. The method has been designed to find a reasonably nearby sounding that is in the “inflow sector” of the event and to reduce the likelihood that the sounding has been contaminated by convection. For example, the lower troposphere may have been stabilized by outflow, the upper troposphere warmed and moistened by anvils, and the wind structure altered radically. For a more thorough examination of the issues related to selecting “proximity soundings” see Brooks et al. (1994a). To accomplish the goal of establishing a sounding as an inflow sector sounding, the boundary layer mean wind vector was computed using the average of the  $u$  and  $v$  wind components in the lowest 500 m. The sounding was assumed to be in the inflow sector of any meteorological event if it was within 400 km and the event fell within  $\pm 75^\circ$  of the boundary layer mean wind vector. This is illustrated in Fig. 1, which shows soundings B and C meeting the inflow and range criteria.

If more than one sounding satisfied the inflow and range criteria, for simplicity the sounding with the largest CAPE was chosen as being “representative” of the event. This was done to alleviate two major problems: with some events, soundings taken in the warm sector, behind the dryline, and north of the warm front in a developing cyclone could all be considered as “inflow” soundings. Further, soundings meeting the inflow and range criteria but contaminated by convection likely have reduced CAPE and thus were more likely to be eliminated. The CAPE criterion sets this study apart from other similar studies and has important implications for the interpretation of the results herein. In any given case, it is quite possible that a sounding with nonzero CAPE that is in close proximity to the event is excluded in favor of a more distant sounding with greater CAPE. From a forecasting perspective, it means that the results herein should be applied in terms of the largest CAPE in a fairly large “inflow region” rather than the CAPE in the immediate storm inflow. Further,

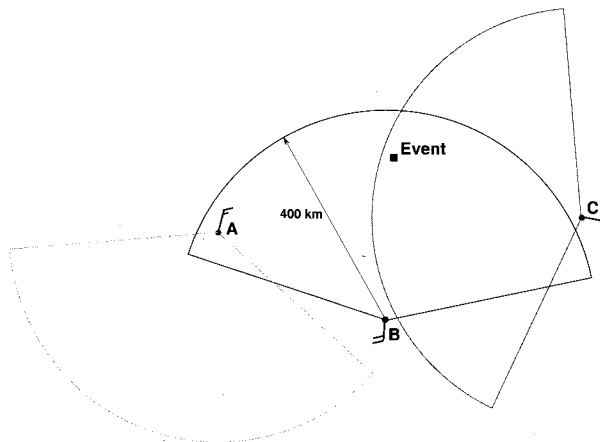


FIG. 1. Schematic illustrating the rules for choosing a representative sounding for an event. Sounding sites are at A, B, C, and the weather event is at the square marked "Event." The boundary layer winds at the sounding sites are denoted using conventional plotting symbols. The "inclusion areas" are the 150° sections with 400-km radius centered on the boundary layer wind vector. The event meets the inclusion criteria for sites B and C, but not A. When more than one sounding meets the criteria, the one with the largest CAPE becomes the representative sounding.

it means that the results herein may not be directly compared to results from similar studies; this point will be reiterated in later sections where appropriate.

Admittedly, the process described above may not be the ideal means of selecting a sounding representative of a meteorological event. A more appropriate method might be to choose only those routine or special soundings that truly were proximate to a given event [e.g., the method of Brooks et al. (1994a)]. Alternatively, one could perform objective analysis or utilize gridded numerical model data to determine the conditions proximate to an event. However, the chosen approach removes all questions about the subjective decisions made in including or excluding various soundings. The "rules" used to associate a sounding with each event are summarized below.

- Step 1: Assemble list of all soundings that are within 400 km of the event.
- Step 2: Assemble the subset of soundings that contain the event in a 150° sector centered on the boundary layer mean wind vector.
- Step 3: Choose the sounding with the maximum CAPE.

After every possible event had a sounding associated with it, the events were tabulated on a sounding-by-sounding basis, giving counts of events associated with each sounding.

### c. Lightning database

Since the primary emphasis of this climatology is on convection, a method was needed to determine which

TABLE 1. Criteria for sounding classification and numbers of soundings.

Category name	No. of soundings	Criteria for association
TOR	51	One or more tornadoes having damage rated as F2 or greater
SUP	119	One or more reports of hail > 5.07 cm (2 in.) diameter, but no tornadoes having damage > F1 (F0, F1 allowed)
ORD	2767	10 or more CGs, but no reports of hail > 5.07 cm diameter, tornadoes of any F rating, nor wind damage allowed

soundings actually were associated with convection and which were not. This is a difficult problem with such a large dataset. The technique chosen was to determine if cloud-to-ground (hereafter CG) lightning flashes were associated with a given sounding. A minimum of 10 flashes was required before the sounding was assumed to be associated with convection.

The CG flash data are from the National Lightning Data Network operated by Geomet Data Services, Inc. All CGs that occurred between 2100 and 0600 UTC (i.e., -3 to +6 h from nominal sounding time) were treated as individual meteorological events, and an attempt was made to find a representative sounding for each one using the rules listed in section 2b. Out of a total of 5 711 187 flashes during the 9-h daily window in all of 1992, 3 748 833 individual CGs (~2/3) were associated with soundings. Based on the rules listed in section 2b, it is apparent that many CGs occurred too far from nonzero CAPE soundings (e.g., far offshore), there were no soundings in the inflow sector of the CG, and, in some cases, there were no nonzero CAPE soundings. No attempt was made to quantify the reasons for CGs not being matched with soundings. Out of 6793 soundings with nonzero CAPE, 2767 were associated with 10 or more CG flashes (see Table 1).

### d. Severe weather reports and classification

The goal of this work is to utilize available data, suitable for a large climatology, to ascertain the association of sounding-derived parameters with severe weather related to supercells. Severe weather reports were taken from Severe Local Storms Unit log for 1992 and were filtered as follows. Tornado reports were filtered into significant (F2 or greater) versus other tornadoes because of the well-known reporting vagaries (e.g., Doswell and Burgess 1988). Only hail larger than or equal to 5.1 cm (2.0 in.) was considered under the assumption that it is associated with supercells when it occurs. Wind reports were not considered in this study because of the difficulty in determining if the severe wind was due to a supercell or not. Only events occurring within -3 to +6 h of 0000 UTC were consid-

ered. These events were matched with soundings using the proximity rules described above.

Three categories of soundings were defined as summarized in Table 1. The categories were designed with the intent to identify soundings associated with tornadic supercells, nontornadic supercells, and nonsupercell storms. Because there is no climatological record of the supercell character of storms, this must be inferred through the available reported phenomena. This requires certain caveats regarding the interpretations and limitations of these categories as described in the following.

**TOR:** This category was designed to identify soundings associated with tornadic supercells. While some of the reports of tornadoes of F2 and greater damage intensity in 1992 possibly were associated with nonsupercell tornadoes, nothing in the database of severe weather reports allows nonsupercell to be distinguished from supercell tornadoes. The justification for the exclusion of F0 and F1 tornadoes in TOR was to generally exclude nonsupercell tornadoes, as well as to filter some of the myriad of erroneous tornado reports (Doswell and Burgess 1988) that generally are given the F0 or F1 rating. The label TOR is used here mainly for convenience; the strict interpretation of the category is *soundings associated with tornadoes rated F2 or greater*.

**SUP:** For comparison to the TOR category, information from the climatological database was sought to identify supercells without significant tornadoes. The only information readily available is reports of large hail in the absence of significant tornadoes. Further research is required to quantify the actual association of large hail with supercells versus nonsupercells, although Cotton and Anthes (1989) state that supercell storms “generally produce the largest hailstones.” It may be determined that the occurrence of large hail is a poor indicator of supercell structure invalidating the present supercell classification. Further, it is likely that many, if not a majority, of supercells do *not* produce hail of the required size and were excluded. The label SUP is used for convenience; the strict interpretation of the category is *soundings associated with storms that produce large hail but not significant tornadoes*, in itself an important category of storms in operational meteorology regardless of the supercell characteristics.

**ORD:** This category was designed to exclude supercells. This was done by including soundings associated with a modest amount of cloud-to-ground lightning, but excluding soundings associated with damaging wind, large hail, or any tornado. This exclusion is based on the idea that most supercells produce some severe weather at the surface (Burgess 1976; Moller et al. 1994).

#### e. Computation of storm motion

In all computations, the assumed storm motion is that computed based on the limited climatology of Rasmus-

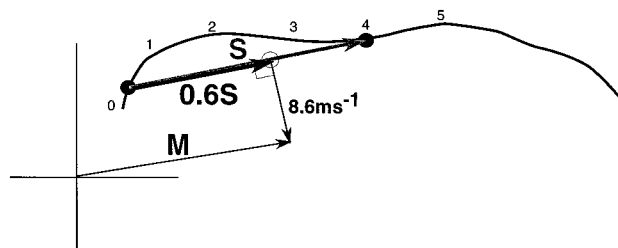


FIG. 2. Illustration of storm motion computation. Hodograph is curve with heights labeled in kilometers. Dots are at the 0–500 m AGL mean and 4 km AGL. Gray vector  $S$  is the BL–4 km shear vector; black vector is  $0.6 S$ . Predicted storm motion vector  $M$  is  $8.6 \text{ m s}^{-1}$  orthogonal to the right of  $0.6 S$ .

sen and Straka (1998). The hodographs for representative soundings for 45 supercell cases were translated so that the 0–500 m above ground level (AGL) (assumed boundary layer, hereafter BL) mean wind was at the origin and rotated so that the BL–4 km AGL shear vector was aligned with the  $+u$  axis. The storm motions were plotted. It was found that for LP (low precipitation updraft region, based on subjective visual classification) and classic supercells, the motion was always within  $4 \text{ m s}^{-1}$  of a point found as follows:  $8.6 \text{ m s}^{-1}$  orthogonal to the right of the tip of the  $0.6S$  vector, where  $S$  is the BL–4 km shear vector (Fig. 2). It is this storm motion vector that is used in the present study and has been tested for several years in the National Center for Atmospheric Research (NCAR) operational version of the Mesoscale Model, version 5, forecast model (J. Bresch 1998, personal communication). Recently, Bunkers et al. (1998) have derived a very similar formula for predicting supercell motion using a sample of 125 supercells based on a technique proposed by M. Weisman (1998, personal communication). Note that unlike the common methods based on angular deviation from deep mean wind vectors, the present method is Galilean invariant. A hodograph produces the same *hodograph-relative* motion regardless of where it falls relative to the origin. In the limited climatology, high precipitation (HP) supercells generally deviated much more than  $4 \text{ m s}^{-1}$  from the “predicted” motion and did not seem to be strongly related to the shear in the lower half of the troposphere. Supercell motion forecasting derived from the above technique, based largely on the work of Rotunno and Klemp (1982), is the subject of an ongoing investigation.

### 3. Shear-related parameters

In this section, the climatology of sounding-derived shear parameters is presented. The computation of specific parameters is described in the appropriate sections. All integrals were computed using the trapezoidal method and the actual reported data. The upper and lower limits of many integrals occur between reported data levels; data at these levels were linearly interpolated (in

TABLE 2. Confidence levels for the multiresponse permutation procedure. Dashes indicate <95% confidence level; only 95% and 99% are shown. Two-dimensional parameters at the bottom (2D) indicate that the test was run in two-dimensions using the two quantities that define the parameter space for that parameter (e.g., SRH and CAPE for EHI).

Parameter	SUP/ ORD	TOR/ ORD	TOR/ SUP
BRN	99	99	—
BL–6-km shear	99	99	—
<i>b</i> Brooks parameter	99	99	—
CAPE	99	99	—
EHI	99	99	95
LCL	99	—	99
Mean shear	99	99	99
SRH	99	99	95
Upper storm-relative wind speed	99	99	—
BRN (2D)	99	99	—
Brooks (2D)	95	99	99
EHI (2D)	99	99	95
VGP (2D)	99	99	95

height) between reported data. Wherever mean values are required, the mean is computed as the average of the values reported weighted by the thickness of the layer represented by that observation (or derived from reported levels) in the sounding. In interpreting the results, it should be noted that the means of the samples in the three categories were examined for statistically significant differences using the *t* test, as well as the more appropriate technique of multiresponse permutation procedures (Mielke et al. 1976; Mielke et al. 1981). In general, the means were statistically significantly different between the three permutations of category pairs, as documented in Table 2.

This section describes the climatology of storm-relative helicity (Davies-Jones et al. 1990), “mean shear” (Rasmussen and Wilhelmson 1983), and storm-relative upper-tropospheric wind speed (Rasmussen and Straka 1998). Several quantities were investigated that did not seem to have significant utility, especially for distinguishing between the TOR and SUP classes of supercells (viz., storm-relative boundary layer wind speed and storm-relative wind speeds every 1000 m in elevation between 3 and 7 km AGL).

*a. Boundary layer to 6-km shear*

In this section, the magnitude of the shear vector between the 0–500 m AGL mean wind and 6 km AGL wind (hereafter BL–6-km shear) is examined. Figure 3 shows the frequency of occurrence of various magnitudes of BL–6-km shear as a function of category. The gray boxes contain the middle 50% of the events, with the median shown with a horizontal black line. The vertical black bar contains the middle 80% of the events. Graphs of this type can be used to gain an understanding of the overall distribution of a parameter, but more importantly they can be used to gauge the relative value

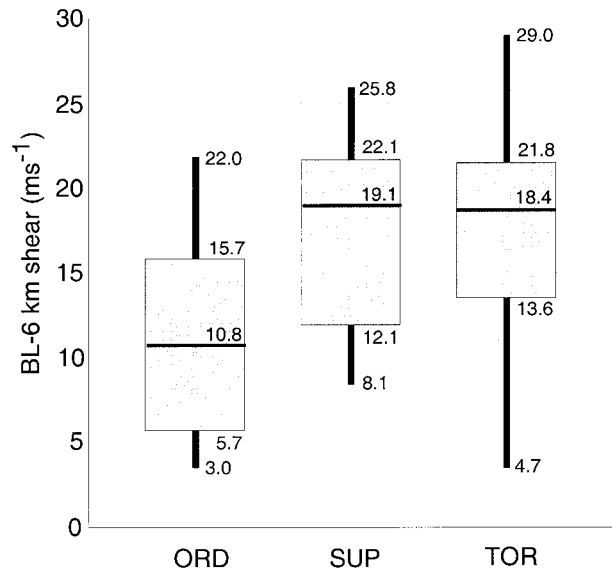


FIG. 3. Box and whiskers graph of BL–6-km shear for soundings associated with supercells with significant tornadoes (TOR; right), supercells without significant tornadoes (SUP; middle), and nonsupercell thunderstorms (ORD; left). Gray boxes denote 25th to 75th percentiles, with heavy horizontal bar at the median value. Thin vertical lines (whiskers) extend to the 10th and 90th percentiles.

of a parameter in distinguishing among categories. It can be seen that BL–6-km shear has value for distinguishing between the populations of soundings associated with the TOR and SUP categories, and that associated with the ORD category. In the case of ORD soundings, BL–6-km shear is between five and 15 m s<sup>-1</sup> in half of the cases, while for TOR–SUP the equivalent range is 11–21 m s<sup>-1</sup>. From Fig. 3 it can also be seen that BL–6-km shear has no utility for distinguishing between the SUP and TOR categories.

*b. Storm-relative helicity*

SRH (Davies-Jones et al. 1990) is defined as

$$SRH = - \int_0^h \mathbf{k} \cdot (\mathbf{V} - \mathbf{c}) \times \frac{\partial \mathbf{V}}{\partial z} dz, \quad (1)$$

where  $\mathbf{V}$  is horizontal velocity,  $\mathbf{c}$  is the storm motion vector, and  $h$  is the depth over which the integration is performed (3 km herein). SRH shows considerably greater utility for distinguishing among the categories than BL–6-km shear (Fig. 4). Most ORD have small SRH (75% with SRH <100 m<sup>2</sup> s<sup>-2</sup>). Half of the SUP soundings have SRH between 64 and 208 m<sup>2</sup> s<sup>-2</sup>. Soundings in the TOR category are quite distinct from the ORD soundings, with no overlap in SRH among the central 50% of cases. The mean value of SRH in TOR soundings is almost 200 m<sup>2</sup> s<sup>-2</sup>. However, it is not true that large SRH implies that a particular sounding will be associated with a significant tornado. The 23% of ORD soundings with SRH between 100 and 168 m<sup>2</sup> s<sup>-2</sup>

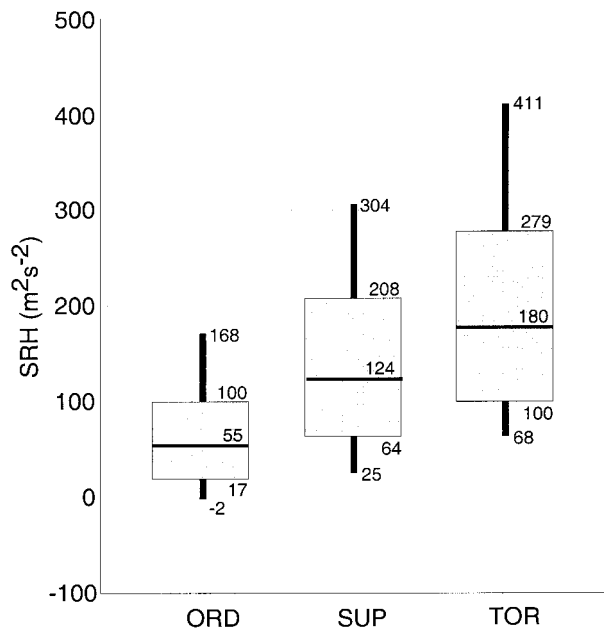


FIG. 4. As in Fig. 3 except for SRH.

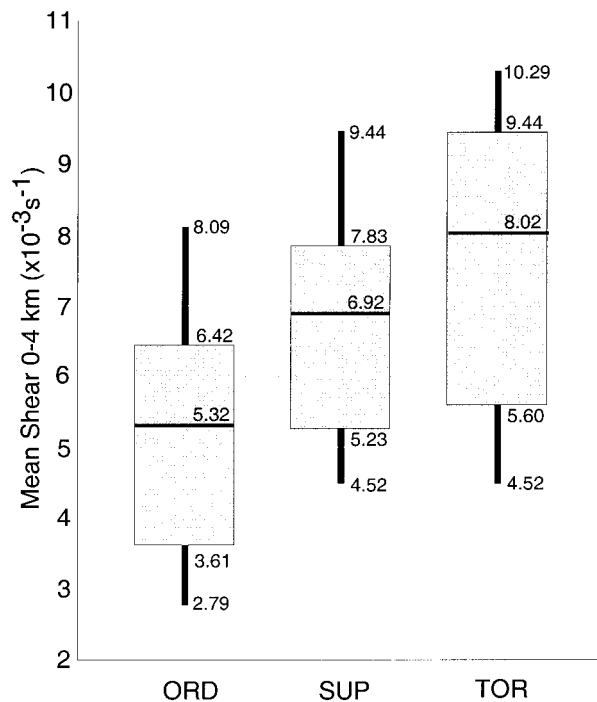


FIG. 5. As in Fig. 3 except for mean shear in the lowest 4 km AGL.

represent over 600 cases, which is more than the total number of soundings in the TOR and SUP categories combined. This “false alarm” problem occurs with all the parameters investigated and will be discussed in section 8.

c. Mean shear

Mean shear (Rasmussen and Wilhelmson 1983) is defined as

$$\bar{S} = \frac{\int_0^h \frac{\partial V}{\partial z} dz}{\int_0^h dz}, \quad (2)$$

which is the length of the hodograph divided by the depth over which the hodograph was measured (4 km here). The box-and-whiskers diagram for mean shear is given in Fig. 5. As with SRH, but to a much smaller degree, mean shear does distinguish between the three categories. For example, half of ORD soundings have mean shear  $<0.053 \text{ s}^{-1}$ , while only 15% of SUP soundings have values that small. Mean shear, as well as SRH, becomes a stronger predictor of supercells and tornadoes when paired with CAPE, as discussed in section 5c. The fact that SRH better discriminates between the categories suggests that it is the streamwise component of horizontal vorticity that dominates the production of rotating updrafts in supercells as described by Davies-Jones (1984).

d. Storm-relative upper-tropospheric wind speed

Recently, Rasmussen and Straka (1998) have evaluated a small (45 case) sample of supercells and concluded that isolated HP supercells (Doswell and Burgess 1993) generally have anvil-level storm-relative wind speeds  $<18 \text{ m s}^{-1}$ , isolated classic supercells have wind speeds between 18 and  $28 \text{ m s}^{-1}$ , and low precipitation (LP) storms are characterized by storm-relative wind speeds  $>28 \text{ m s}^{-1}$  [see Rasmussen and Straka (1998) and references therein for a more complete discussion of these supercell types and the climatological analysis]. Here, we evaluate the storm-relative winds for the 2-km-deep layer centered at the  $-40^\circ\text{C}$  level in the sounding (Fig. 6). Average upper-tropospheric flow strength is greater in the SUP sounding population than in the ORD. This may indicate that the strong low-level shear favoring supercells continues through the depth of the sounding, or it may be an indication that supercells do indeed require a certain amount of storm-relative upper-tropospheric flow to evacuate the water mass that diverges from the updraft summit. The Rasmussen and Straka (1998) finding that isolated HP supercells exist in environments with upper-tropospheric storm-relative wind speeds  $<18 \text{ m s}^{-1}$  would suggest that at least half of all supercells should be HP based on the data shown in Fig. 6. Because the Rasmussen and Straka analysis is for supercells that are isolated from “seeding” effects of nearby storms it can be inferred that the typical occurrence of nearby storms implies that even more supercells should be HP than the  $\sim 1/2$  implied above.

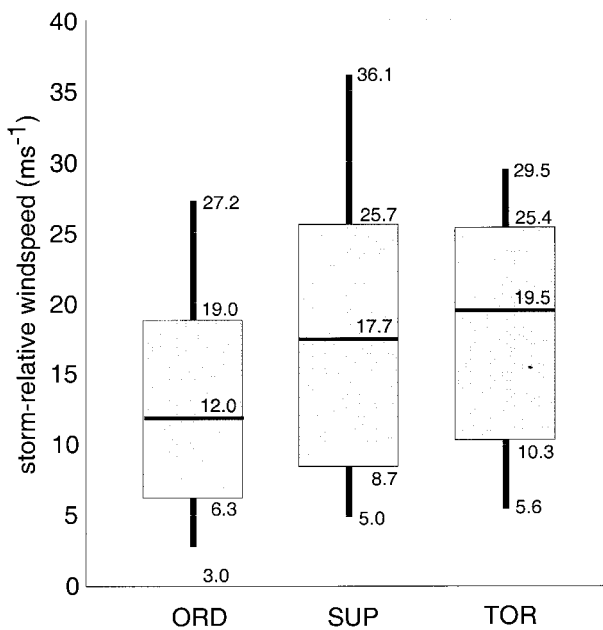


FIG. 6. As in Fig. 3 except for storm-relative upper-tropospheric wind speed.

Therefore this climatology, combined with the notion that many supercells are driven toward the HP end of the spectrum by seeding, is consistent with the observation that a majority of supercells are indeed HP storms (Moller et al. 1994).

#### 4. Parameters related to CAPE

##### a. CAPE

CAPE (Moncrieff and Miller 1976) is in common use as a forecast tool for supercells. It is included here as a guide to aid forecasters in understanding what constitutes large or “extreme” CAPE as often quoted in National Weather Service forecast discussions. In this investigation, the virtual temperature correction has been included (Doswell and Rasmussen 1994), and the parcel has the uniformly mixed equivalent potential temperature of the lowest 1000 m of the atmosphere. If one assumes that extreme refers to those ORD soundings composing the upper 10% of the distribution, then CAPE  $\geq 1820 \text{ J kg}^{-1}$  is extreme in this sample. Fifty percent of the ORD soundings have CAPE  $\geq 530 \text{ J kg}^{-1}$  (Fig. 7). Interestingly, CAPE is significantly different between ORD and SUP soundings, as well as between ORD and TOR soundings, suggesting that CAPE alone has some value as a supercell predictor, even when not paired with a measure of shear (although combined measures are much better, as discussed below). The reader is urged to remember that the CAPE values may be biased upward compared to actual proximity values owing to the use of the sounding with the largest CAPE when more than one meets the inflow sector criterion.

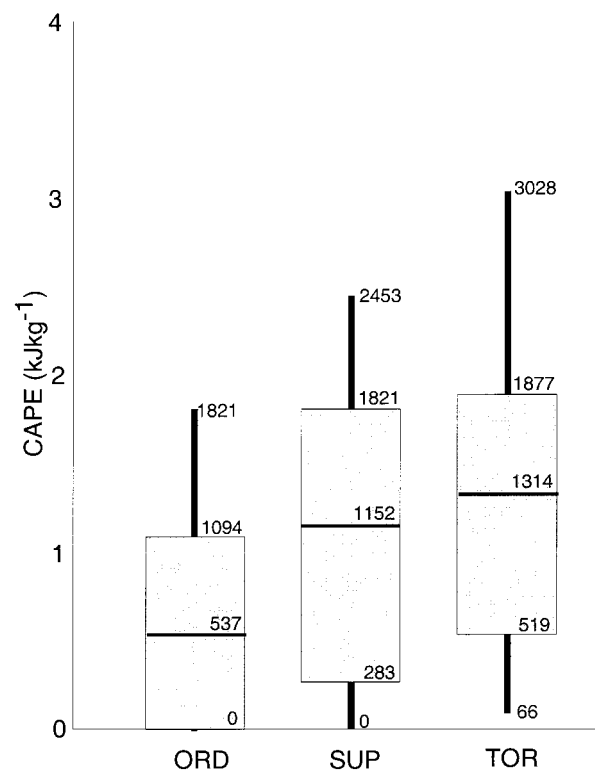


FIG. 7. As in Fig. 3 except for CAPE.

##### b. CAPE immediately above the LFC

Consistent with the idea that large low-level stretching is required for low-level mesocyclone intensification and perhaps tornadogenesis, several researchers have explored the idea that the distribution of CAPE with height is important and large low-level accelerations are favorable for tornadic supercells (McCaul 1991). Figure 8 depicts the distribution of the CAPE that accrues in the soundings in the lowest 3 km above the level of free convection (LFC). It appears that the ORD category has somewhat less CAPE in the lowest 3 km of buoyancy than the two supercell categories, consistent with the previous finding that this category has less CAPE in general. Very little difference can be seen between the TOR and SUP categories, contradicting the idea that increased low-level stretching, perhaps associated with significant tornadoes, owes to low-level CAPE. Instead, the required stretching probably can be attributed to dynamic pressure effects from the interaction of low-level shear and the updraft.

##### c. Downdraft CAPE

Owing to the apparent association of the rear-flank downdraft (RFD) with tornadogenesis (Lemon and Doswell 1979), and more recent work by Gilmore and Wickner (1998) on the role of midlevel dryness in supercell downdraft production, downdraft CAPE (dCAPE) was

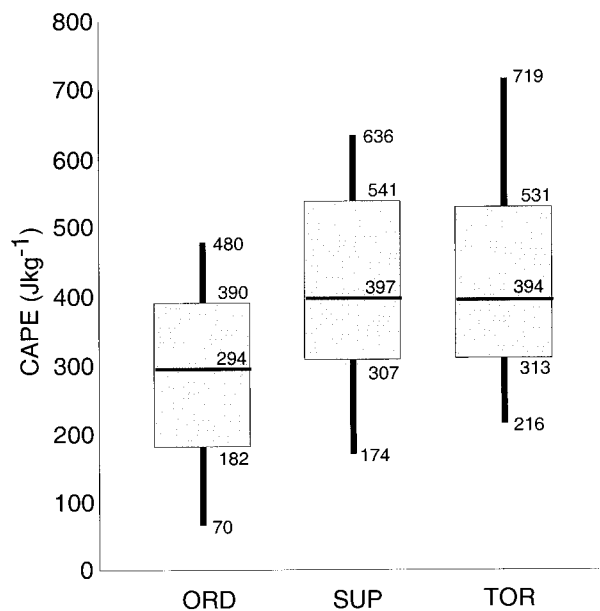


FIG. 8. As in Fig. 3 except for CAPE in the first 3 km above the LFC.

investigated. Downdraft sources at levels spaced 1 km apart beginning at 1 km AGL were examined. None of these showed any clear differences between the categories in terms of the frequency distributions. There are various possible causes for this null finding. It is possible that the RFD is not driven primarily by negative buoyancy, but is instead caused by accelerations associated with nonhydrostatic vertical pressure gradient forces [e.g., the “occlusion downdraft” of Klemp and Rotunno (1983) or downward forcing associated with pressure increases in the midlevel stagnation region upwind of the updraft]. Further, it is possible, as suggested by Gilmore and Wicker (1998) that the appropriate parameter space for forecasting RFD intensity includes low-level shear as well as dCAPE. The association of the RFD with sounding-derived parameters is discussed further in section 8.

## 5. Shear–CAPE combinations

### a. Bulk Richardson number

The bulk Richardson number (BRN) has been used as a supercell predictor ever since it was investigated using numerical simulations (Weisman and Klemp 1982). Weisman and Klemp determined that environments with  $BRN < 50$  favored supercells, while  $BRN > 50$  favored multicellular events. The parameter space of CAPE and BL–6-km shear is shown in Fig. 9. Supercells (TOR and SUP; all circles) are generally found at larger CAPE and BL–6-km shear than nonsupercells (ORD; dots). The frequency density contours were computed by gridding the parameter space and dividing the number of soundings in each grid cell by the total num-

ber of soundings of that category. The heavy black contour representing higher probabilities of SUP is considerably displaced toward larger CAPE and shear than the equivalent probability of ORD. This implies that the “correct” combination of CAPE and shear for discriminating between SUP and ORD is of the form  $CAPE^x$  times shear<sup>y</sup>, where  $x$  and  $y$  are both positive, rather than 1.0 and  $-0.5$  as in the BRN.

Combining these two parameters into a form of the BRN yields the distributions shown in Fig. 10. The range of BRN suggested by Weisman and Klemp for supercells does appear to be validated by this climatology with over 75% of the SUP soundings having  $BRN < 17$ . However, over 50% of ORD soundings have these values as well, meaning that BRN is a poor discriminator (compared to EHI and VGP below) between supercell and nonsupercell sounding populations. It was found that the BRN as formulated by Weisman and Klemp (1982), using the density-weighted mean wind from the surface to 6 km instead of the 6-km wind itself, has similar capability to discriminate among the categories.

### b. Energy–helicity index

The energy–helicity index (EHI) (Hart and Korotky 1991; Davies 1993) is defined as

$$EHI = \frac{(CAPE)(SRH)}{1.6 \times 10^5}. \quad (3)$$

This index is used operationally for supercell and tornado forecasting, with values larger than 1.0 indicating a potential for supercells, and  $EHI > 2.0$  indicating a large probability of supercells. The EHI parameter space of CAPE and SRH for this climatology is shown in Fig. 11. As with BRN, but to a greater degree, it can be seen that TOR and SUP soundings occupy a different portion of the parameter space than ORD soundings, with the primary differences being that the former have larger SRH. Further, it appears that EHI has some value in discriminating between TOR and SUP soundings. Although further research is required, this is in contrast to the finding by Brooks et al. (1994a) that combinations of CAPE and shear do not discriminate between tornadic and nontornadic supercells (significant differences in the sizes of the datasets and the methodology may account for this disagreement). In fact, the likelihood of significant tornadoes does increase with increasing EHI, as shown in Fig. 12. Based on this climatology, it appears that EHI is a good discriminator between all three populations of soundings (see additional discussion in section 9). For ORD soundings, 90% have  $EHI < 0.77$ , while only about 60% of SUP soundings have  $EHI < 0.77$ , and less than  $\frac{1}{3}$  of TOR soundings have values less than 0.77. TOR soundings are very strongly distinguished in the neighborhood of  $EHI = 1.5$ , where  $\sim 50\%$  of TOR supercells have values greater than 1.5

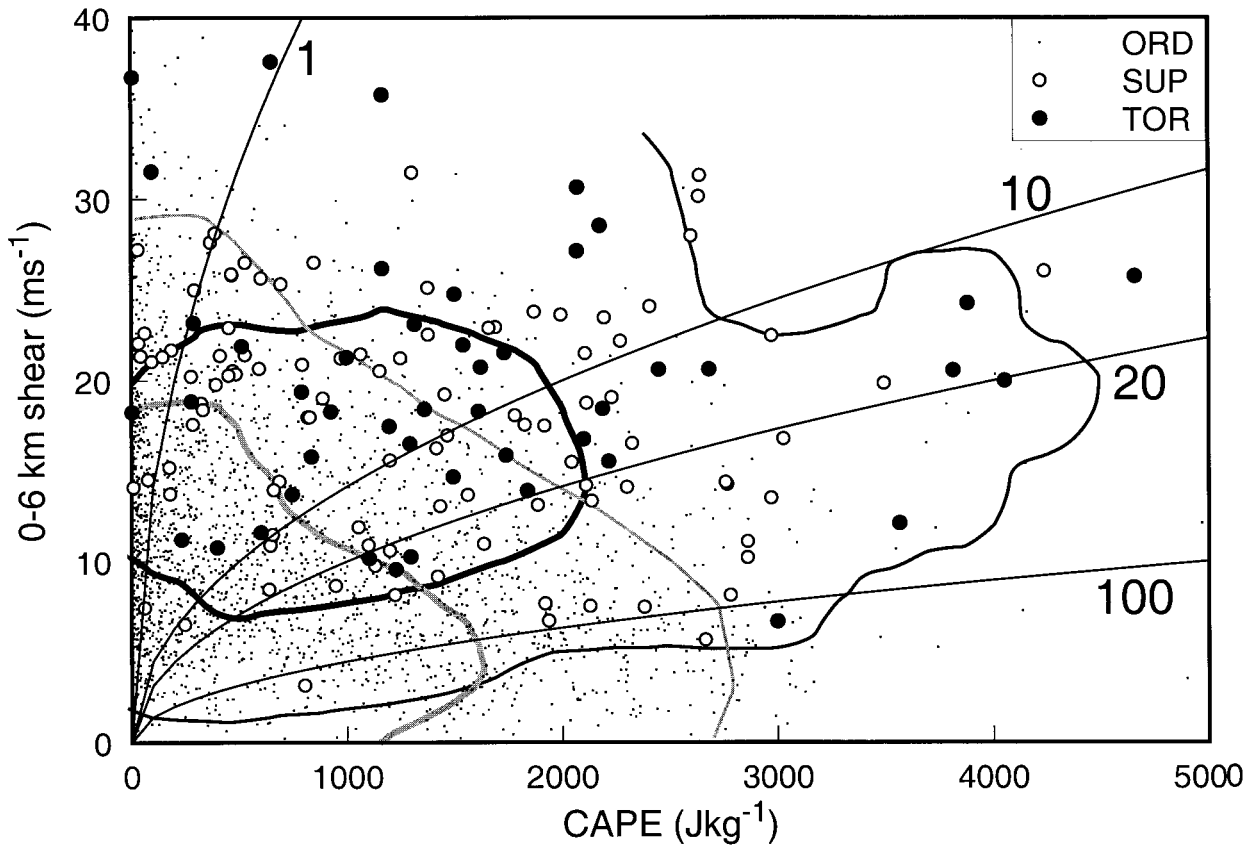


FIG. 9. Scatter diagram of soundings representing supercells with significant tornadoes (TOR; solid circles), without significant tornadoes (SUP; open circles), and nonsupercell thunderstorms (ORD; dots). Labeled curves are lines of constant BRN. Thick contours are lines of constant frequency density (see text); heavy contours represent  $1 \times 10^{-5} \text{ (m s}^{-1} \text{ J kg}^{-1})^{-1}$  and thin contours  $2 \times 10^{-6} \text{ (m s}^{-1} \text{ J kg}^{-1})^{-1}$ ; gray is for ORD and black is for TOR.

and only 10% of SUP soundings have values larger than 1.5.

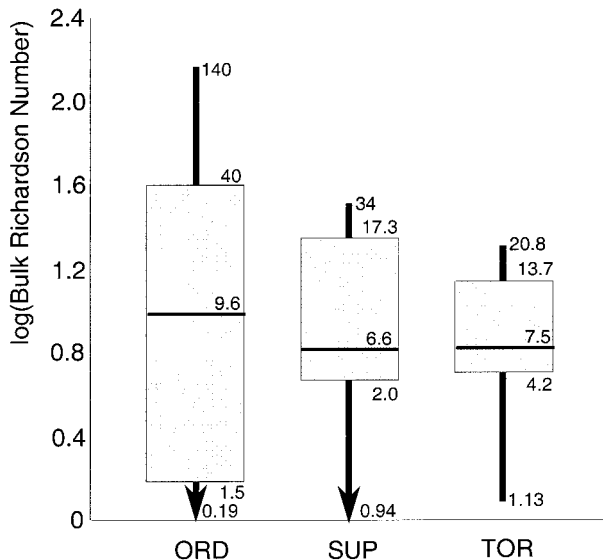


FIG. 10. As in Fig. 3 except for BRN.

c. Vorticity generation parameter

The vorticity generation parameter (VGP) is derived from an examination of the parameter space investigated in Rasmussen and Wilhelmson (1983) and the physical concept of tilting of vorticity. The rate of conversion of horizontal to vertical vorticity through tilting is

$$\left(\frac{\partial \zeta}{\partial t}\right)_{\text{tilt}} = \eta \cdot \nabla w, \tag{4}$$

where  $\zeta$  is the vertical component of vorticity,  $\eta$  is the horizontal vorticity vector, and  $w$  is the vertical component of velocity. Here,  $\text{VGP} = [S(\text{CAPE})^{1/2}]$ , where  $S$  is mean shear (or hodograph length divided by depth [Eq. (2)]). To the extent that mean shear is proportional to  $\eta$ ,  $w$  is proportional to  $\text{CAPE}^{1/2}$ , and storm updrafts are all of roughly the same horizontal scale, VGP is roughly proportional to the tilting rate in Eq. (4). Figure 13 illustrates the CAPE and mean shear parameter space. As with EHI, in general the SUP and TOR sound-

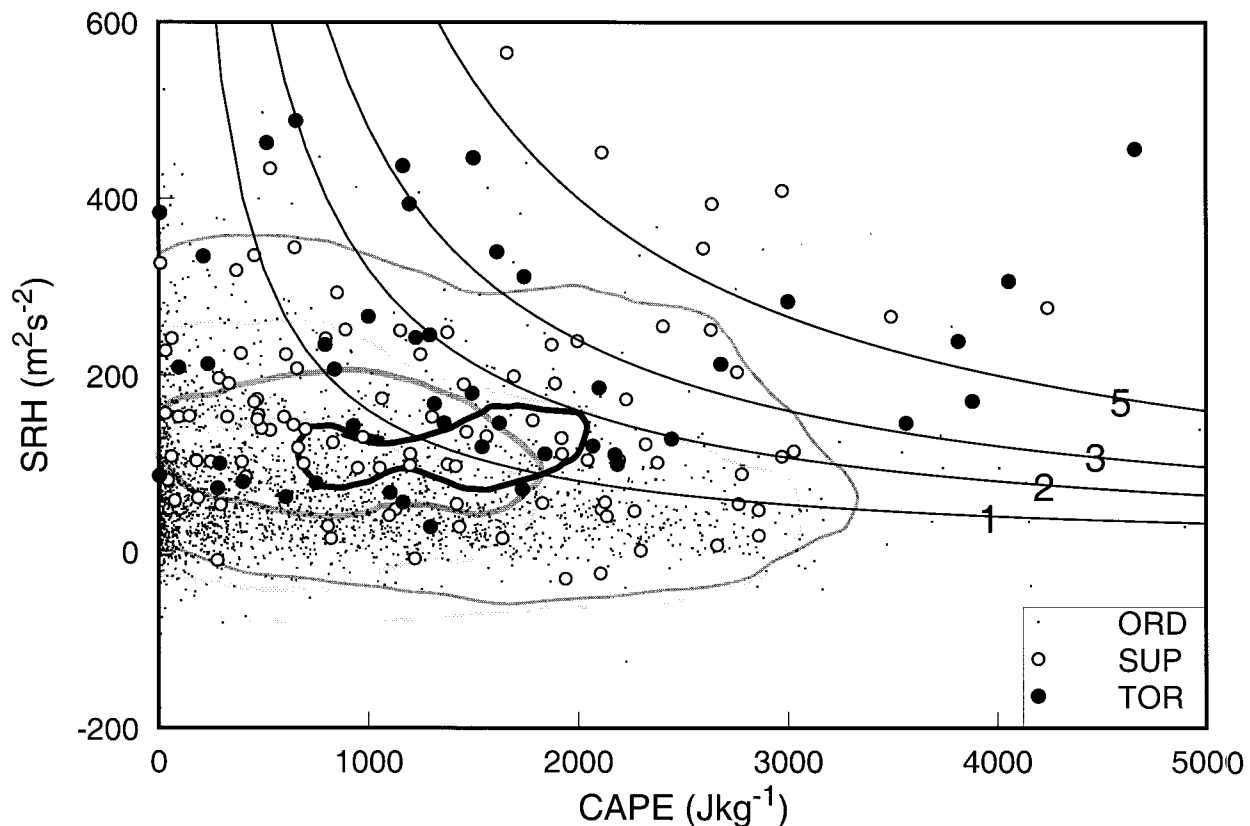


FIG. 11. As in Fig. 9 except for EHI. Labeled curves are lines of constant EHI. Probability density contours are for probability of  $2 \times 10^{-7} (\text{m}^2 \text{s}^{-2} \text{J kg}^{-1})^{-1}$  (thin contours),  $1 \times 10^{-6} (\text{m}^2 \text{s}^{-2} \text{J kg}^{-1})^{-1}$  (heavy contours), and black for TOR, medium gray for SUP, and light gray for ORD. Thin black contour omitted.

ings occupy a different part of the parameter space than ORD soundings. These differences are further illustrated by examining the box-and-whiskers diagram of VGP (Fig. 14). Like EHI (but to a slightly lesser degree), the mean values of VGP are significantly different between all three categories of soundings. Further, as with EHI, TOR soundings have an obviously different frequency distribution than SUP soundings.

In summary, the combination of CAPE and shear in VGP and EHI substantially improves the use of soundings in discriminating among the three categories compared to the various measures of shear or CAPE alone. BL-6-km shear distinguishes the population of supercell soundings from nonsupercells. However, it would appear that low-level shear, especially the streamwise component of horizontal vorticity paired with CAPE, plays a more important role in the production of significant tornadoes.

## 6. Low-level thermodynamics

### a. Lifting condensation level

The lifting condensation level (LCL) was investigated in this climatology because the authors have observed on a number of occasions that supercells on hot days,

with adequate CAPE and shear, failed to produce tornadoes and seemed to be characterized by too much outflow. This was found to occur even in the presence of  $\text{CAPE} > 4000 \text{ J kg}^{-1}$ . It is hypothesized that relatively low values of boundary layer relative humidity support more low-level cooling through the evaporation of rain, leading to stronger outflow. Relatively dry boundary layers are characterized by higher LCLs. The distributions in Fig. 15 are consistent with the subjective storm intercept observations. In fact, it can be seen that the LCL on TOR soundings is significantly lower than that for SUP soundings, and even somewhat *lower than that for nonsupercells* (ORD). Half of the TOR soundings have LCLs below 800 m, while half of the SUP soundings have LCLs above 1200 m. It should be noted that with the LCL, as with most of the parameters explored herein, major variation occurs on small time- and space scales (e.g., Markowski et al. 1998b) that are not well sampled with network soundings. Actual LCL heights near tornadic supercells may be considerably lower than found here.

### b. Convective inhibition

There are at least two plausible reasons why convective inhibition (CIN; Colby 1984) might be related to

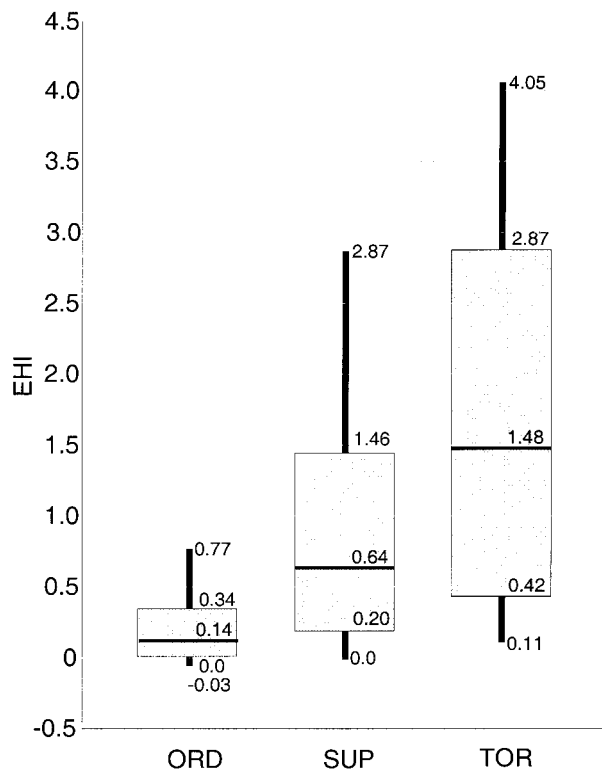


FIG. 12. As in Fig. 3 except for EHI.

the occurrence of supercells and tornadoes. First, the presence of large CIN in soundings *associated with thunderstorms* would tend to indicate that the thunderstorms are being strongly forced by local low-level convergence (e.g., by a cold front, outflow). Local strong forcing could imply that storms would tend to be organized into larger-scale convective systems rather than isolated supercells that are more favorable for tornadoes. Second, supercells occurring with large CIN could be “elevated” storms (Colman 1990) that draw inflow from a potentially buoyant layer above the boundary layer; these storms are thought to be relatively less likely to produce tornadoes. Because the occurrence of elevated storms in this climatology is unknown, the association of these events with the large CIN soundings is also unknown.

In this analysis, three-fourths of soundings associated with significant tornadoes occur with  $\text{CIN} < 21 \text{ J kg}^{-1}$ , whereas over 60% of SUP soundings had CIN *larger* than this value (Fig. 16). This topic merits further research before it can be considered for operational application; the findings herein should be considered preliminary and the explanations speculative.

## 7. Parameter space of helicity, mixing ratio, and midlevel storm-relative wind speed

A final parameter space merits evaluation via the climatology. Brooks et al. (1994a) evaluated a smaller cli-

matology of proximity soundings (using a much different definition) for a particular tornadogenesis “failure mode.” A related modeling study (Brooks et al. 1994b) suggested that water loading near the mesocyclone produced too much outflow, leading to tornadogenesis failure. This situation was found to result from an imbalance between mesocyclone strength (related to the rate of advection of precipitation around the back of the updraft) and storm-relative midlevel flow (related to the rate at which hydrometeors are drawn away from the updraft). In evaluating the model results, Brooks et al. (1994a) examined the parameter space of low-level mixing ratio versus the quotient of SRH and minimum midlevel storm-relative wind speed in the 2–9 km AGL layer. Low-level mixing ratio was thought to be important because numerical simulations had indicated that rain production near the updraft increased with increasing mixing ratio.

Herein, the same parameter space is examined for the 1992 sounding climatology (Fig. 17), with the caveat that Brooks et al. used maximum SRH in the lowest 3 km, whereas the present study uses the value at 3 km AGL. Also, the Brooks et al. (1994a) study used maximum mixing ratio whereas the present analysis uses mean mixing ratio in the lowest 1000 m AGL. These differences are thought to be minor, but the differences in category definition (e.g., Brooks et al. included all tornadoes and this study includes tornadoes  $\geq \text{F2}$ ) and proximity preclude direct comparison of the results. Instead, the goal here is to evaluate this set of parameters in the context of the TOR, SUP, and ORD classifications.

The lines in Fig. 17 are equivalent to those in Fig. 5 of Brooks et al., although they should probably be shifted upward and to the right to account for the differences in computations noted above. With such a shift, it appears that this parameter space does discriminate to some degree between TOR and SUP categories (recall Brooks et al. looked at mesocyclones with *any* tornadoes and those without). Because the straight lines shown in Fig. 17 (using the slopes proposed by Brooks et al.) do seem to partition the present parameter space, a new variable,  $b$ , is introduced here<sup>1</sup> to obtain a more quantitative analysis of the differences in the populations in this parameter space. This variable is constant along the lines shown in Fig. 16 and is given by

$$b = q + c \log \left( \frac{\text{SRH}}{V_{\min}} \right), \quad (5)$$

where  $c = 11.5$ ,  $q$  is the mean mixing ratio and  $V_{\min}$  is the minimum midlevel wind speed. The distributions of

<sup>1</sup> It is suggested that the reader heed the advice of Brooks et al. (1994a) and avoid the use of “magic numbers” in severe weather forecasting. The variable  $b$  is introduced solely as an analysis tool, not as a forecast parameter. The emphasis of this paper is to gain new physical insight into large-scale influences on supercells, not to promote magic-number approaches to forecasting.

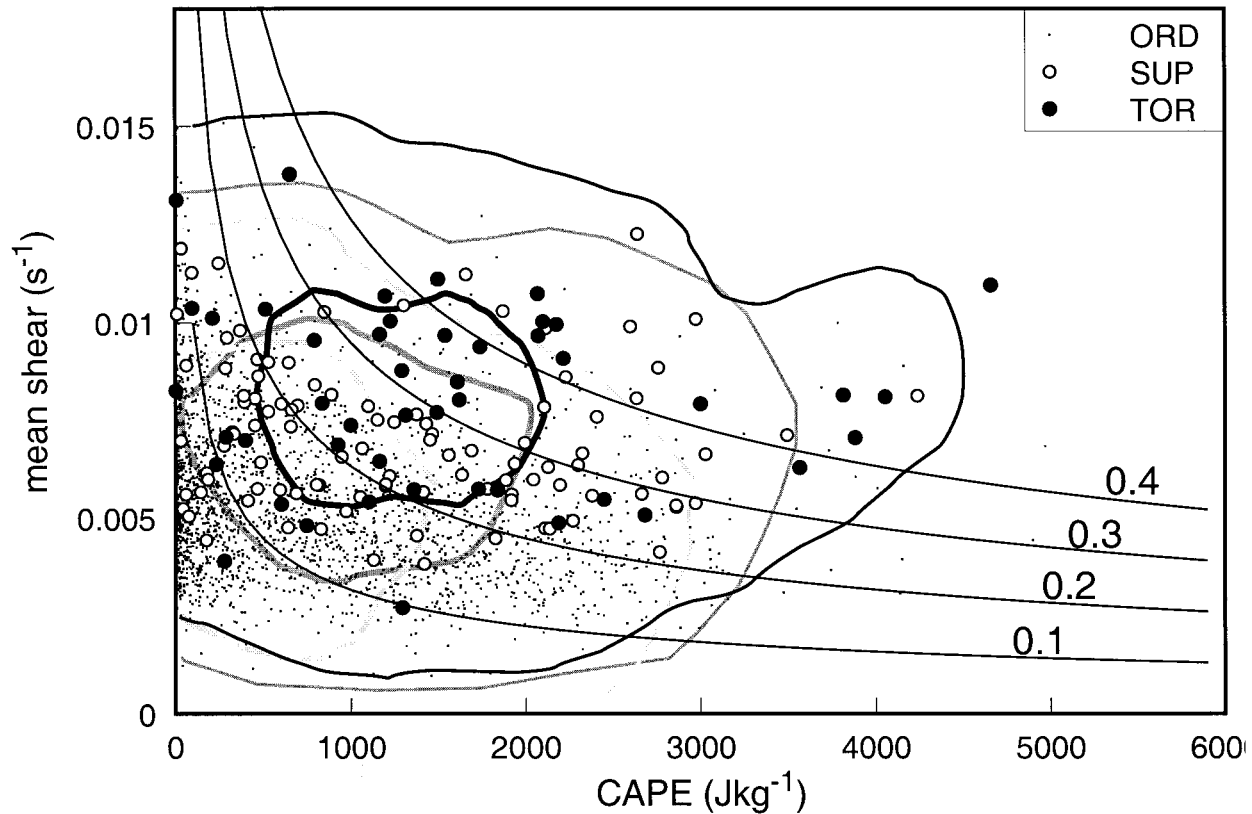


FIG. 13. As in Fig. 9 except for CAPE vs mean shear. Labeled curves are lines of constant VGP. Probability density contours are for probability of  $6 \times 10^{-3} \text{ (s}^{-1} \text{ J kg}^{-1}\text{)}^{-1}$  (thin contours),  $3 \times 10^{-2} \text{ (s}^{-1} \text{ J kg}^{-1}\text{)}^{-1}$  (heavy contours), and black for TOR, medium gray for SUP, and light gray for ORD.

b for this climatology are shown in Fig. 18. Compared to the distributions of EHI and VGP it can be seen that the distributions are much less well separated, with a great degree of overlap among the middle 50% of the cases in each category. This would suggest that this particular combination of parameters is a relatively

poorer discriminator among the present categories (see section 8), although the difference in means is significantly different at the 95% confidence level in all comparisons. The discrimination possibly improves when all tornadoes are considered instead of just significant tornadoes as examined herein (C. Doswell 1998, personal communication).

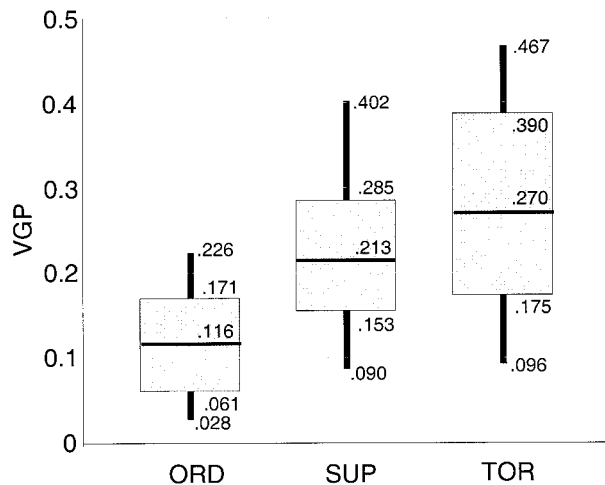


FIG. 14. As in Fig. 3 except for VGP.

### 8. Objective comparison of forecast utility

In the previous sections, various subjective comparisons between forecast parameters were given. The primary purpose of this investigation has been to motivate further research and provide baseline climatological values for various parameters. However, in this section an objective method for comparing forecast utility is developed.

The Heidke's skill score [HSS; for a summary of numbers related to forecast skill based on the  $2 \times 2$  contingency table see Marzban and Stumpf (1998)] is used to assess the relative forecast accuracy of the various parameters. Doswell et al. (1990) demonstrate that the HSS is superior to the critical success index (CSI) for evaluating forecasts of rare events because it gives credit for a correct forecast on a nonevent. To examine

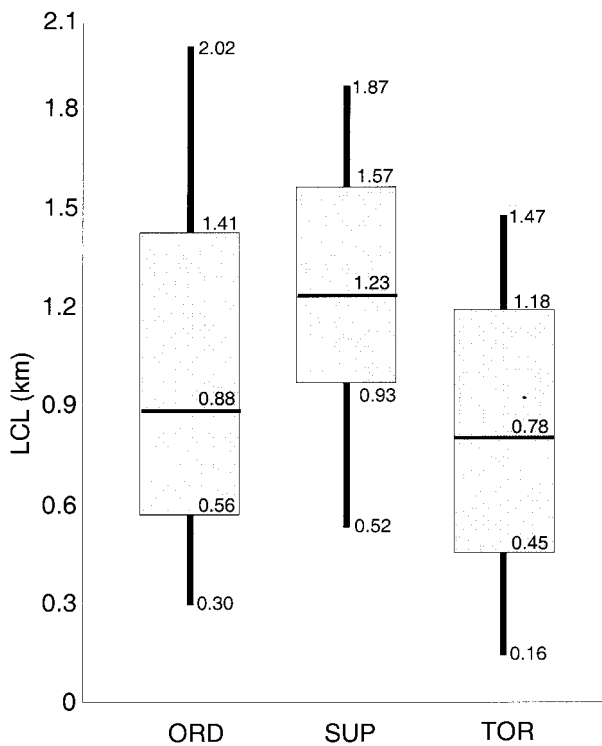


FIG. 15. As in Fig. 3 except for LCL.

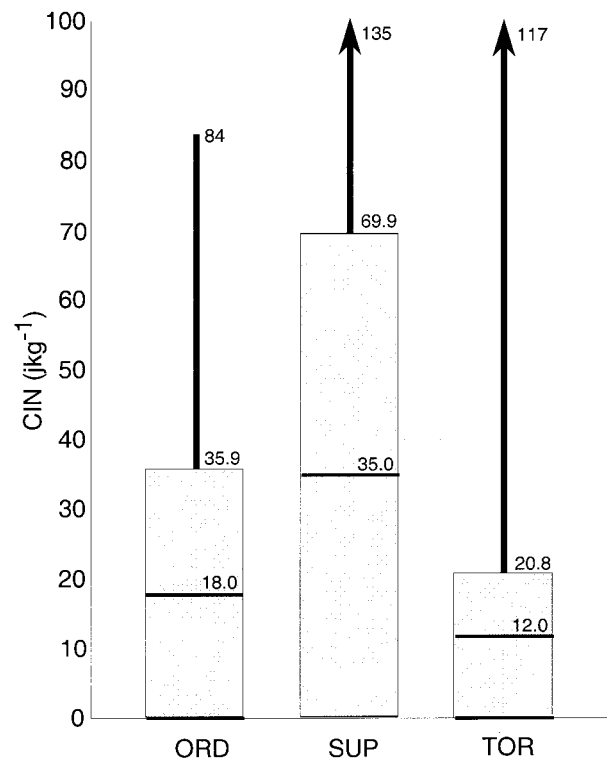


FIG. 16. As in Fig. 3 except for CIN.

the ability of a parameter to forecast the occurrence of TOR versus SUP storms, the following rule is used: given that a sounding is associated with the occurrence of large hail or a significant tornado (union of SUP and TOR), if the value of the parameter is greater than  $x$ , then a significant tornado will be associated with the sounding. The value of  $x$  that maximizes the HSS for this rule is sought. This value,  $x_{opt}$ , is found by examining HSS for all possible  $x$ . The value of the parameter at  $x_{opt}$  is termed the optimal value for the parameter.

A graph illustrating the behavior of the false alarm ratio (FAR), probability of detection (POD), CSI, and HSS for the parameter VGP is shown in Fig. 19. The HSS has a much more prominent peak than the CSI, which barely exceeds the “CSI no-skill” level (the CSI that is achieved for a forecast that TOR will occur for any sounding with  $VGP > 0$ ). This behavior is true in general. This probably is an indication of the validity of the findings of Doswell et al. (1990) regarding forecast accuracy measures for rare events.

As one comparative, objective test of the usefulness of these parameters in the TOR versus SUP forecast problem, parameters are ranked and HSS is summarized in Table 3. It is interesting that the parameter that shows the most utility for discriminating between TOR and SUP soundings is LCL height. Of the combined CAPE and shear parameters, VGP has the best HSS by a small margin.

A similar analysis can be performed to gauge the

utility of the parameters for forecasting supercells given thunderstorms. The specific rule is this: given the occurrence of 10 or more CGs associated with a sounding there will be large hail or a tornado associated with the sounding (SUP or TOR) if the value of the parameter is greater than  $x$ . The optimal HSS values are summarized in Table 4. The “best” parameter for distinguishing between supercells and ORD, using this measure of forecast utility, is EHI, with the other shear/CAPE combination (VGP) being second best.

## 9. Summary

One issue not discussed thus far is that even for relatively strong discriminators for supercells, such as EHI and VGP, the false alarm rate is very high. For example, consider a value of EHI (Fig. 12) of 4.0. Only about 10% of soundings with significant tornadoes have EHI larger than this, so it would seem that this number should mean a very high probability of tornadoes. About 99% of nonsupercell soundings have  $EHI < 4.0$ , but the remaining 1.2%, with  $EHI > 4.0$ , comprise 33 soundings, while the 10% of significant tornado soundings comprise only six soundings. In other words, at an EHI of 4.0, only about 6/45 of the soundings was associated with significant tornadoes (an additional 6/45 soundings were SUP).

There are a number of reasons why this large false alarm rate is present in this climatology. The most likely

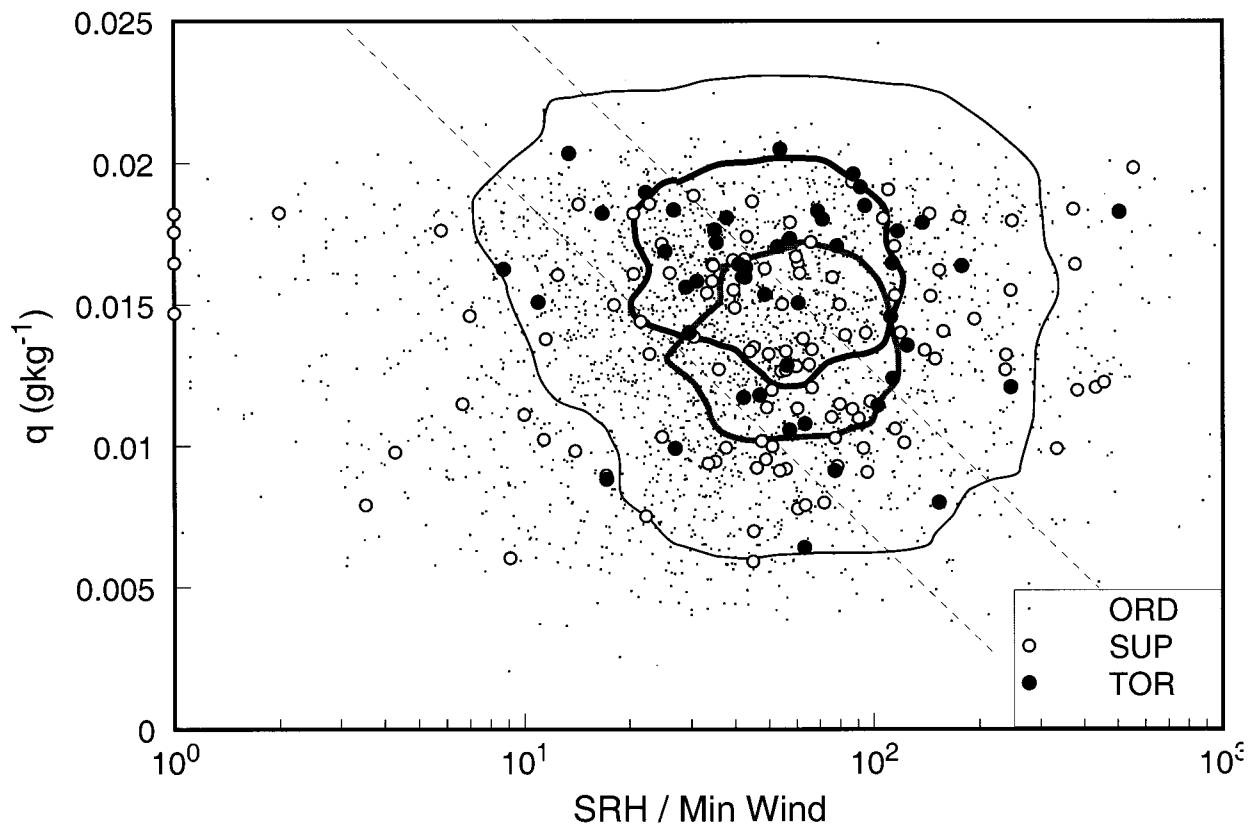


FIG. 17. As in Fig. 9 except for the ratio of SRH minimum midlevel storm-relative wind speed vs low-level mixing ratio ( $q$ ). Dashed lines are lines of constant  $b$ . Probability density contours are for probability of  $12 \text{ (m s}^{-3} \text{ g kg}^{-1})^{-1}$  (thin contours),  $60 \text{ (m s}^{-3} \text{ g kg}^{-1})^{-1}$  (heavy contours), and black for TOR, and medium gray for SUP.

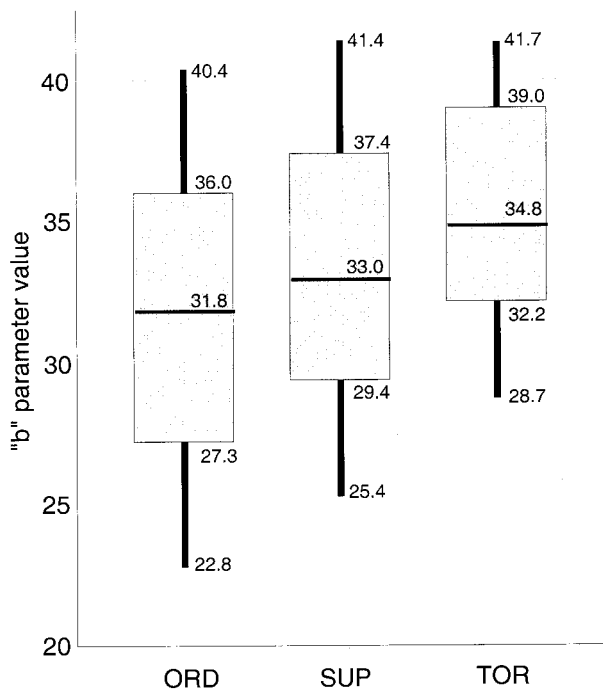


FIG. 18. As in Fig. 3 except for the parameter  $b$  derived from the Brooks et al. (1994a) parameter space.

reason is that there are factors that militate against supercells even when the soundings suggest that large-scale conditions favor them. The mode of convection is not well understood at this time and may not be readily forecastable using soundings. Strong larger-scale forcing, tending to organize convection into quasi-two-dimensional lines (without supercells), may decrease the likelihood of supercells even when soundings indicate

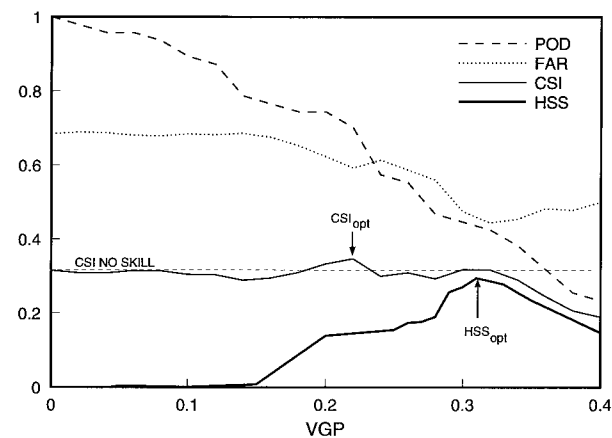


FIG. 19. Graph of FAR, POD, CSI, and HSS for the VGP.

TABLE 3. Parameters ranked according to Heidke's skill score in the TOR vs SUP forecast when HSS &gt; 0.15.

Parameter	Optimal HSS	Optimal value
LCL	0.348	800 m
CIN	0.297	16 J kg <sup>-1</sup>
VGP	0.295	0.31
EHI	0.267	1.05
Mean shear	0.247	0.009 s <sup>-1</sup>
SRH	0.176	200

TABLE 4. Parameters ranked according to Heidke's skill score in the (SUP + TOR) vs ORD forecast when HSS &gt; 0.15.

Parameter	Optimal HSS	Optimal value
EHI	0.386	1.40
VGP	0.315	0.280
SRH	0.268	230 m <sup>2</sup> s <sup>-2</sup>
Mean shear	0.227	0.00963 s <sup>-1</sup>
BL-6-km shear	0.189	20.5 m s <sup>-1</sup>
CAPE	0.179	2100 J kg <sup>-1</sup>

that conditions are favorable. Similarly, deep tropospheric flow that is largely parallel to low-level "trigger" mechanisms is known to result in solid lines of convection instead of isolated cells.

Inadequate reporting of severe weather events could also contribute to this problem. However, this is a minor effect in this climatology because only one report in a fairly large area is needed to classify a sounding as SUP or TOR.

It is also possible that in many cases the soundings that appeared favorable for supercells and significant tornadoes really were not representative of the inflow to the actual nonsupercell events that occurred. This would imply that the smaller-scale, unsampled regions near the storms themselves typically are less favorable for severe storms than the larger-scale environment that is being sampled in this climatology. For example, if numerous storms occur and their outflows interfere or combine in such a way to reduce the CAPE or low-level shear, perhaps supercells are prevented. Recent research (e.g., Markowski et al. 1998b) has focused on mesoscale phenomena that enhance the probability of supercells and tornadoes; perhaps there are other phenomena that locally decrease the probability.

However, there is another distinct possibility: perhaps the larger-scale environment almost never contains sufficient conditions for tornadic supercells. This has been suggested in the recent work by Markowski et al. (1998a) and Markowski et al. (1998b) in which it is shown, for example, that mesoscale and storm-scale augmentations of helicity to values above 300 m<sup>2</sup> s<sup>-2</sup>, and sometimes much larger (doubling to quadrupling the ambient, larger-scale value), are associated with tornadic supercells. Perhaps in the present climatology, the significant tornadoes occurred when enough "mesoscale augmentation" was present, but in the majority of cases such augmentation did not occur. If this is the case, then sounding information can only delineate if conditions are *generally* favorable for supercells and/or tornadoes, and the forecaster must focus on mesoscale features, such as baroclinic boundaries, that locally could enhance supercell or tornado potential significantly. If this hypothesis is found to be correct, it is not, however, clear why EHI (for example) is substantially greater on the large scale in soundings associated with significant tornadoes. It would seem that local augmentations, by storms or mesoscale features, must *amplify* preexisting

favorable shear and perhaps CAPE [just such a scenario has been documented in Richardson et al. (1998, manuscript submitted to *Mon. Wea. Rev.*) for the 2 June 1995 tornado outbreak in west Texas].

It has been shown herein that the most valuable tools for distinguishing between SUP and ORD are combinations of low-level shear and CAPE (such as EHI or VGP). The height of the LCL can add additional useful information for the TOR versus SUP decision, with LCL heights above about 1200 m AGL associated with decreasing likelihood of significant tornadoes.

In this study, attention was focused on possible failure modes of tornadogenesis in order to distinguish between soundings supporting supercells with or without significant tornadoes. Numerous parameters were examined that could be important in RFD formation, using the hypothesis that lack of an RFD, or an RFD that is too strong (Brooks et al. 1994b), could preclude tornado formation. The Brooks et al. (1994a) parameter space was explored and only weakly discriminated between the two populations (SUP and TOR). The value of downdraft CAPE at all levels from 1 to 6 km was investigated assuming that evaporative cooling drives the RFD; these parameters did not distinguish among the categories. Storm-relative wind speed at the same heights was examined under the assumption that stagnation of flow produces a downward-directed net pressure gradient force leading to an RFD; these parameters also did not distinguish among the categories. This null finding permits the hypothesis that it is the low-level pressure deficit associated with a near-ground mesocyclone that drives the RFD (Klemp and Rotunno 1983). This is consistent with the finding that as EHI or VGP become large, presumably leading to stronger mesocyclones, the likelihood of significant tornadoes increases. However, much research remains to be done in order to understand RFD dynamics and tornadogenesis failure.

Other failure modes were discussed herein. It appears that too much outflow, whether or not it was associated with the RFD, could be decreasing the likelihood of significant tornadoes in supercells. This is one possible explanation for the finding that LCL height is generally larger in soundings associated with SUP versus TOR.

Future work will involve expanding this climatology to a multiyear study. This will enable the examination of the interannual variability of sounding parameters and

the associated variability of the frequency of severe events. As new hypotheses are developed regarding the failure of supercells to produce significant tornadoes, these will be tested. Additional research is required to determine if soundings contain useful information regarding the likely character of RFDs and whether they will form. Additional research is also required to determine if the organization of convection can limit the potential for supercells and tornadoes in environments with otherwise favorable shear and CAPE. Finally, additional research is needed to determine if, in fact, mesoscale and storm-scale enhancements to generally favorable large-scale conditions are usually required to produce supercells and/or significant tornadoes.

*Acknowledgments.* Partial support for this research was provided by the National Science Foundation through Grant ATM-9617318. Additional support was provided by NOAA through a Presidential Early Career Award for Scientists and Engineers. The authors are grateful for the careful review and constructive criticisms of Drs. Brooks, Doswell, and Davies-Jones of NSSL; Mr. Albert Pietrycha of NCAR; as well as two anonymous reviewers.

## REFERENCES

- Bluestein, H. B., and C. R. Parks, 1983: A synoptic and photographic climatology of low-precipitation severe thunderstorms in the southern plains. *Mon. Wea. Rev.*, **111**, 2034–2046.
- , and M. H. Jain, 1985: Formation of mesoscale lines of precipitation: Severe squall lines in Oklahoma during the spring. *J. Atmos. Sci.*, **42**, 1711–1732.
- , and S. S. Parker, 1993: Modes of isolated, severe convective storm formation along the dryline. *Mon. Wea. Rev.*, **121**, 1354–1372.
- , G. T. Marx, and M. H. Jain, 1987: Formation of mesoscale lines of precipitation: Nonsevere squall lines in Oklahoma during the spring. *Mon. Wea. Rev.*, **115**, 2719–2727.
- Brooks, H. B., C. A. Doswell III, and J. Cooper, 1994a: On the environments of tornadic and nontornadic mesocyclones. *Wea. Forecasting*, **9**, 606–618.
- , —, and R. B. Wilhelmson, 1994b: The role of midtropospheric winds in the evolution and maintenance of low-level mesocyclones. *Mon. Wea. Rev.*, **122**, 126–136.
- Bunkers, M. J., B. A. Klimowski, J. W. Zeitler, R. L. Thompson, and M. L. Weisman, 1998: Predicting supercell motion using hodograph techniques. Preprints, *19th Conf. on Severe Local Storms*, Minneapolis, MN, Amer. Meteor. Soc., 611–614.
- Burgess, D. W., 1976: Single-Doppler radar vortex recognition. Part I: Mesocyclone signatures. Preprints, *17th Conf. on Radar Meteorology*, Seattle, WA, Amer. Meteor. Soc., 97–103.
- Colby, F. P., 1984: Convective inhibition as a predictor of convection during AVE-SESAME-2. *Mon. Wea. Rev.*, **112**, 2239–2252.
- Colman, B. R., 1990: Thunderstorms above frontal surfaces in environments without positive CAPE. Part I: A climatology. *Mon. Wea. Rev.*, **118**, 1103–1121.
- Cotton, W. R., and R. A. Anthes, 1989: *Storm and Cloud Dynamics*. Academic Press, 883 pp.
- Darkow, G. L., and M. G. Fowler, 1971: Tornado proximity wind sounding analysis. Preprints, *Seventh Conf. on Severe Local Storms*, Kansas City, MO, Amer. Meteor. Soc., 148–151.
- Davies, J. M., 1993: Hourly helicity, instability, and EHI in forecasting supercell tornadoes. Preprints, *17th Conf. on Severe Local Storms*, St. Louis, MO, Amer. Meteor. Soc., 107–111.
- , and R. H. Johns, 1993: Some wind and instability parameters associated with strong and violent tornadoes. 1. Wind shear and helicity. *The Tornado: Its Structure, Dynamics, Prediction, and Hazards, Geophys. Monogr.*, No. 79, Amer. Geophys. Union, 573–582.
- Davies-Jones, R. P., 1984: Streamwise vorticity: The origin of updraft rotation in supercell storms. *J. Atmos. Sci.*, **41**, 2991–3006.
- , 1993: Helicity trends in tornado outbreaks. Preprints, *17th Conf. on Severe Local Storms*, St. Louis, MO, Amer. Meteor. Soc., 56–60.
- , D. Burgess, and M. Foster, 1990: Test of helicity as a tornado forecast parameter. Preprints, *16th Conf. on Severe Local Storms*, Kananaskis Park, AB, Canada, Amer. Meteor. Soc., 588–592.
- Doswell, C. A., III, and D. W. Burgess, 1988: On some issues of United States tornado climatology. *Mon. Wea. Rev.*, **116**, 495–501.
- , and —, 1993: Tornadoes and tornadic storms: A review of conceptual models. *The Tornado: Its Structure, Dynamics, Prediction, and Hazards, Geophys. Monogr.*, No. 79, Amer. Geophys. Union, 161–172.
- , and E. N. Rasmusson, 1994: The effect of neglecting the virtual temperature correction on CAPE calculations. *Wea. Forecasting*, **9**, 625–629.
- , R. Davies-Jones, and D. L. Keller, 1990: On summary measures of skill in rare event forecasting based on contingency tables. *Wea. Forecasting*, **5**, 576–585.
- Gilmore, M. S., and L. J. Wicker, 1998: The influence of midtropospheric dryness on supercell morphology and evolution. *Mon. Wea. Rev.*, **126**, 943–958.
- Hart, J. A., and W. Korotky, 1991: The SHARP workstation v1.50 users guide. National Weather Service, NOAA, US. Dept. of Commerce, 30 pp. [Available from NWS Eastern Region Headquarters, 630 Johnson Ave., Bohemia, NY 11716.]
- Johns, R. H., J. M. Davies, and P. W. Leftwich, 1993: Some wind and instability parameters associated with strong and violent tornadoes. 2. Variations in the combinations of wind and instability parameters. *The Tornado: Its Structure, Dynamics, Prediction, and Hazards, Geophys. Monogr.*, No. 79, Amer. Geophys. Union, 583–590.
- Kerr, B. W., and G. L. Darkow, 1996: Storm-relative winds and helicity in the tornadic thunderstorm environment. *Wea. Forecasting*, **11**, 489–505.
- Klemp, J. B., and R. Rotunno, 1983: A study of the tornadic region within a supercell thunderstorm. *J. Atmos. Sci.*, **40**, 359–377.
- Lemon, L. R., and C. A. Doswell III, 1979: Severe thunderstorm evolution and mesocyclone structure as related to tornadogenesis. *Mon. Wea. Rev.*, **107**, 1184–1197.
- Maddox, R. A., 1976: An evaluation of tornado proximity wind and stability data. *Mon. Wea. Rev.*, **104**, 133–142.
- Markowski, P. M., E. N. Rasmusson, and J. M. Straka, 1998a: The occurrence of tornadoes in supercells interacting with boundaries during VORTEX-95. *Wea. Forecasting*, **13**, 852–859.
- , J. M. Straka, E. N. Rasmusson, and D. O. Blanchard, 1998b: Variability of storm-relative helicity during VORTEX. *Mon. Wea. Rev.*, **116**, 2959–2971.
- Marzban, C., and G. J. Stumpf, 1998: A neural network for damaging wind prediction. *Wea. Forecasting*, **13**, 151–163.
- McCaul, E. W., Jr., 1991: Buoyancy and shear characteristics of hurricane-tornado environments. *Mon. Wea. Rev.*, **119**, 1954–1978.
- Mielke, P. W., K. J. Berry, and E. S. Johnson, 1976: Multi-response permutation procedures for a priori classifications. *Commun. Stat. Theor. Meth.*, **A5**, 1409–1424.
- , —, and G. W. Brier, 1981: Application of multi-response permutation procedures for examining seasonal changes in monthly mean sea-level pressure patterns. *Mon. Wea. Rev.*, **109**, 120–126.
- Moller, A. R., C. A. Doswell III, M. P. Foster, and G. R. Woodall, 1994: The operational recognition of supercell thunderstorm environments and storm structures. *Wea. Forecasting*, **9**, 327–347.
- Moncrieff, M., and M. J. Miller, 1976: The dynamics and simulation

- of tropical cumulonimbus and squall lines. *Quart. J. Roy. Meteor. Soc.*, **102**, 373–394.
- Rasmussen, E. N., and R. B. Wilhelmson, 1983: Relationships between storm characteristics and 1200 GMT hodographs, low-level shear, and stability. Preprints, *13th Conf. on Severe Local Storms*, Tulsa, OK, Amer. Meteor. Soc., J5–J8.
- , and J. M. Straka, 1998: Variations in supercell morphology. Part I. Observations of the role of upper-level storm-relative flow. *Mon. Wea. Rev.*, **126**, 2406–2421.
- Rotunno, R., and J. B. Klemp, 1982: The influence of the shear-induced pressure gradient on thunderstorm motion. *Mon. Wea. Rev.*, **110**, 136–151.
- Taylor, G. E., and G. L. Darkow, 1982: Atmospheric structure prior to tornadoes as derived from proximity and precedent upper air soundings. NRC Tech. Rep. NUREG/CR-2359, 95 pp.
- Weisman, M. L., and J. B. Klemp, 1982: The dependence of numerically simulated convective storms on vertical wind shear and buoyancy. *Mon. Wea. Rev.*, **110**, 504–520.